A wavelet based invigoration check in fingerprint scanners

Aditya Abhyankar, *Member, IEEE,* and Stephanie Schuckers

Abstract— It has been shown that fingerprint scanners can be deceived easily, using simple, inexpensive techniques. In this work, countermeasure against such attacks is suggested, that utilizes a novel wavelet based approach to detect liveness associated with fingerprint scanners. Liveness is determined from perspiration changes along the fingerprint ridges, observed only in live people. The algorithm utilizes two images captured over time and is divided into pre-processing steps, wavelet analysis, and post-processing steps. The pre-processing steps include image enhancement techniques. Wavelet analysis is performed separately for low and high frequency data. Daubechies filters (N=16) are designed generating scale and wavelet functions. Post-processing involves sub-band alignment and energy distribution analysis. The normalized energy content of significant wavelet coefficients (those changing more than 40 % from the first to second image) is used as a measure to perform liveness classification. The proposed algorithm was applied to a data set of approximately 58 live, 50 spoof and 28 cadaver fingerprint images captured at 0 sec and 2 or 5 sec, from each of three different types of scanners, namely optical (Secugen), capacitive DC (Precise Biometrics) and optoelectrical (Ethentica). The algorithm provides a method for improved spoof protection by complete classification of live fingers from not live fingers.

Index Terms— fingerprints, spoofing, liveness, wavelet analysis, multiresolution analysis, wavelet packet analysis, energy distribution analysis.

I. INTRODUCTION

With more efficient communication techniques and more complex networked societies, human recognition has gained significance. Biometrics is defined as "automated methods for verifying or identifying the identity of a living individual based on physiological or behavioral characteristics" [1]. Biometrics has advantages over traditional identifiers like identity cards, signatures etc., in that they can not be forgotten, transferred, misplaced, duplicated, or stolen easily [1], [2]. Some examples of biometric identifiers include fingerprints, iris, hand geometry, voice, speech, face and gait. Fingerprints are the oldest, most studied and most widely used [3].

Fraudulent entry of an unauthorized person into a fingerprint recognition system by using faux fingerprint sample is termed spoofing [4]. Recently different spoofing techniques have been reported, which include fake fingers using gelatin (gummy

fingers), moldable plastic, clay, play-doh, wax, and silicon, developed from casts of live fingers or latent fingerprints [4], [5], [6], [7], [8], [9]. Cadaver fingers have also been shown to reliably be scanned and verified by fingerprint devices of various technologies [4]. One efficient countermeasure against such a fraudulent attacks is liveness detection. As the name suggests, this technique checks whether the incoming biometric signal is coming from a live, genuine person [4], [10], [9].
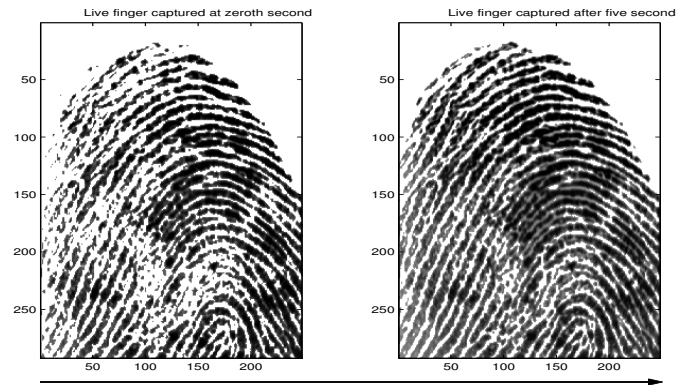

Fig. 1. Live fingerprint images captured as a time sequence. The left figure is captured immediately after placement of finger on the scanner (zeroth second), while the right is captured after five seconds. Perspiration is observed as time progresses.

It has been demonstrated that perspiration can be used as a measure of liveness detection for fingerprint matching systems [8], [11]. Unlike cadaver or spoof fingers, live fingers demonstrate a distinctive spatial moisture pattern, when in physical contact with the capturing surface of the fingerprint scanner. As shown in figure (1), this pattern evolves in time due to the physiological phenomenon of perspiration, and hence, can be called a 'perspiration pattern'. A signal processing-based method has been developed previously, which formulates one-dimensional ridge signal and uses different classification methods like back propagation neural network, One R and discriminant analysis. This method is capable of producing classification rates in the range of 45% to 90% for several scanner technologies [4],[8]. A new wavelet based approach is proposed which is capable of classifying live fingers from not live fingers. Two-dimensional discrete wavelet techniques analyze and extract the significant information from images captured as time series. Distinct separation of the energy bands is obtained and hence no classifier is required. Compared to the algorithm given in [8], the proposed algorithm uses the entire two-dimensional image.

II. Wavelet based algorithm

The complete algorithm can be divided into three parts. The first part includes pre-processing steps to prepare the data for the wavelet analysis. The second part is the actual wavelet analysis. Post processing steps to perform classification form the third part.

A. Pre-processing steps

1) Data management: Data previously collected in our lab is used to test the algorithm. This data set is diverse as far as age, sex, and ethnicity is concerned. Different age groups (23 people between ages 20-30 years, 18 people between 30-40, 9 people between 40-50, and 8 people greater than 50), ethnicities (Asian-Indian, Caucasian, Middle Eastern), and approximately equal numbers of men and women are represented. The data was collected using three different fingerprint scanners, with different underlying technologies including: optical (Secugen model FDU01), electro-optical (Ethentica model Ethenticator USB 2500) and capacitive DC (Precise Biometrics model PS100) techniques of capturing a fingerprint. For spoof finger images, a cast was made from each live subject using dental material and spoofs were created from Play-Doh using the procedure given in [8]. Images from cadaver subjects were collected in collaboration with the Musculoskeletal Research Center at West Virginia University (WVU). Protocols for data collection from the subjects were followed that were approved by the West Virginia University Institutional Review Board (IRB) (HS#14517 and HS#15322). Three images were collected as a time-series live scan, at 0 seconds after placement, 2 seconds or 5 seconds. For the algorithm, two images were used. From here on, the image captured at zeroth second will be referred as the 'first' image, and the images captured after 2 seconds or 5 seconds will be referred as the 'second' image. The algorithm was tested for both the combinations. The data set consists of 130 to 136 fingerprints from live, spoof, and cadavers, depending on the scanner used. Table (I) summarizes the available data. Differences in the number of images per scanner are due to inclusion criteria which requires an accepted enrollment image within five tries. Image collection was performed using custom software developed from device SDKs. All algorithm development was performed using MATLAB.

TABLE I

Data set: Distribution

	Capacitive DC Precise Biometric	Electro-optical Ethentica	Optical Secugen
Live	58	55	58
Spoof	50	50	52
Cadaver	33	22	28

2) Image enhancement: Two raw images captured by a biometric scanner at the zeroth second and after two or five seconds are selected for use in the algorithm. These images are converted to suitable format before further processing. Before doing wavelet analysis, it is necessary to enhance the images using histogram equalization and median filtering. The major reasons are as follows:

- Captured images may not be clean because of the dust on the fingers or due to the latent finger impressions deposited on the scanner surface.
- The images could be of varying average contrast, due to the varying pressures at the time of the capture.
- The images could be too faint or too dark depending upon whether the finger is too dry or too sweaty.

Median Filtering: A median filter is a smoothing filter. The ultimate result is noise reduction, but at the cost of sharpness. The filter substitutes the values of each pixel with the median of itself and each adjacent pixel including diagonals. Figure (2-a) shows the original image. Figure (2-b) shows the image after median filtering. In order to show the result of median filtering, histograms are shown in figures (2-c) and (2-d), before and after, respectively. The bottom left figure shows two peaks. The left peak is the noise, and is seen removed in the right bottom figure.
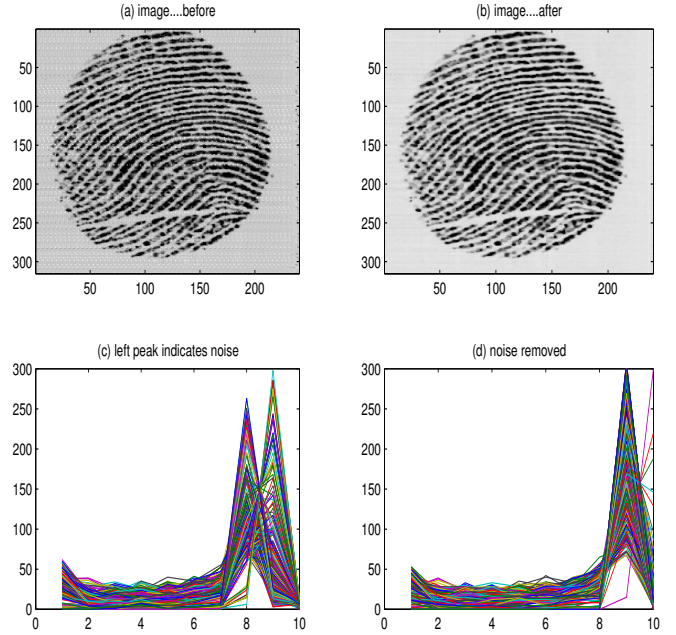

Fig. 2. Median Filtering. Figure (a) shows the original image. Figure (b) shows image after median filtering. in order to show the result of median filtering, histograms are shown in figures (c) and (d), before and after respectively. There are 10 different density regions, and hence x-axis varies from 0 to 10. The original image size is 310×240, and so the 310 different values are plotted on the y-axis. The bottom left figure shows two peaks. The left peak is the noise, and is seen removed in the right bottom figure.

Histogram Equalization: From the histogram of an image, an estimate of the cumulative density function (CDF) is obtained by summing the bin values from 1 to n bins for the nth bin. As the input image is digital and eight bit, n ranges from 1 to 256. The output image has improved contrast. This essentially means a wider range of gray levels, or more even distribution of the gray levels, or both.

B. Wavelet analysis

After the images are enhanced, the perspiration pattern is isolated by using wavelet analysis. The basic steps of the

algorithm are to perform the wavelet transform of the first and last images, select the most important coefficients through maxima energy extraction, calculate MRA for low frequency components and wavelet packet analysis for high frequency components. Once processed, further post-processing gives the perspiration pattern and liveness measure, described in the next section. This section is divided into filter design, wavelet transform implementation, maxima energy extraction, multiresolution, and wavelet packet analysis.

1) Filter Design: For this particular algorithm, Daubechies wavelet is selected as the mother wavelet. This is in accordance with the following properties of Daubechies wavelets [12]:

- orthonormality, having finite support.
- optimal, compact representation of the original signal from a sub-band coding point of view, thus producing multiresolution effect.
- capability to select maximum vanishing moments and minimum phase, so as to extract even minute details from smoother parts.
- cascade algorithm which can zoom-in on particular features of ϕ.

Daubechies filters used for this algorithm are designed so that the phase of the filter is minimum and the number of vanishing moments are maximum. This is of particular importance as not all the images are well focused and it is crucial to extract the changing information even from the smoother parts of the images.

The main focus of the implementation is to construct compactly supported wavelets ψ [12], [13]. The scaling function ϕ itself is chosen to have compact support, hence it automatically ensures the compact support of wavelet ψ.

For compactly supported ϕ, the 2π periodic function h_o becomes a trigonometric polynomial [12].

The orthonormality of the $\phi_{0,n}$ implies:

$$|h_o(\xi)|^2 + |h_o(\xi + \pi)|^2 = 1. \tag{1}$$

The Equation (1) in z domain is as follows:

$$|H(z)|^2 + |H(-z)|^2 = 1 \quad all \quad |z| = 1 \tag{2}$$

Let N be the length of the filter to be designed. Then, $(N/2) - 1$ degrees of freedom are used to obtain maximum vanishing moments $k = N/2$.

The filter is designed for N=16 and k=8. To design Daubechies filters $Q(z)$ is an intermediary step to calculate $H(z)$.

$$
\begin{aligned}
(|Q(z)|)^2 &= \sum_0^{k-1} \left(\binom{(N/2) - 1 + k}{k} (\frac{2 - z - z^{-1}}{4})^k \right) \tag{3} \\
&= \sum_0^7 \left(\binom{15}{8} (\frac{2 - z - z^{-1}}{4})^8 \right) \tag{4}
\end{aligned}
$$

The roots of equation (3) and the retained roots to formulate the minimum phase filter are given in table (II). The value of the constant is calculated using $Q(e^{jw}) = 1$ at $w = 0$ and was found to be 0.0544 after scaling.

TABLE II
DAUBECHIES MINIMUM PHASE FILTER DESIGN

Roots of equation 3	Retained roots	
2.7367	-	
2.5296 + 0.8198i	-	
2.5296 − 0.8198i	-	
1.9388 + 1.4558i	-	
1.9388 − 1.4558i	-	
1.0380 + 1.7304i	-	
1.0380 − 1.7304i	-	
0.2549 + 0.4250i	*	(z_1)
0.2549 − 0.4250i	*	(z_1^*)
0.3298 + 0.2476i	*	(z_2)
0.3298 − 0.2476i	*	(z_2^*)
0.3577 + 0.1159i	*	(z_3)
0.3577 − 0.1159i	*	(z_3^*)
0.3654	*	(z_4)
* = retained roots		

$$H(z) = (\frac{1 + z}{2})^k Q(z) \tag{5}$$

$Q(z)$ is substituted in equation (5) to find $H(z)$ and ultimately $h(n)$, the analysis low pass filter. As these are the orthogonal filters, the remaining filters are obtained from the analysis low pass filter. For example, the analysis high pass filter is obtained by inverting the analysis low pass, and negating the alternate values. Both synthesis filters are obtained by inverting the analysis filter vectors and cross labelling.

The designed filters are shown in figure (3). For our algorithm, the filters are designed for the number of coefficients to be 16. This number is found to be the best trade-off between smoothness of the filters and computational time.
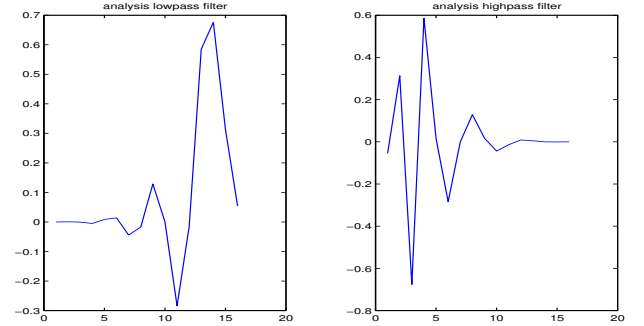

Fig. 3. Daubechies analysis filters. The left figure shows the low pass filter and the right figure shows high pass filter. The filters are designed for the number of coefficients to be 16. X axis indicates the coefficient number, while the Y axis shows the value for that coefficient number. The filter is normalized so that sum of all the filter coefficients is equal to $\sqrt{2}$.

As stated earlier, scale and wavelet functions, ϕ and ψ, are compactly supported L^2 functions, satisfying

$$\phi(x) = \sqrt{2} \sum_n h_n \phi(2x - n) \tag{6}$$

$$\psi(x) = \sqrt{2} \sum_n (-1)^n h_{-n+1} \phi(2x - n) \tag{7}$$

The designed ϕ and ψ functions are shown in figure (4). The $\psi_{j,k}(x) = 2^{-j/2}\psi(2^{-j}x - k), j, k \in Z$ forms a tight frame of

$L^2(R)$, which is an orthonormal basis [12]. Implementation of ψ and ϕ is done in MATLAB (v6.5-R13). At the heart of implementation is the operation of convolution.
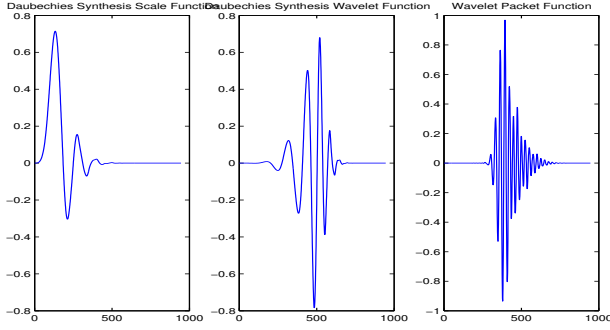

Fig. 4. Left figure indicates Daubechies scale function (ϕ), middle figure indicates Daubechies wavelet function (ψ), and right figure shows the wavelet packet function. For all figures, the number of iterations are selected to be 5.

2) Wavelet transform: The algorithm of wavelet transform implementation revolves around following equation,

$$f_j(x) = \sum_k \alpha_{j,k} 2^{\frac{j}{2}} \phi(2^j x - k) + \sum_k \beta_{j,k} 2^{\frac{j}{2}} \psi(2^j x - k) \quad (8)$$

where, $\alpha_{j,k} = \int f_j(x) 2^{\frac{j}{2}} \phi(2^j x - k) dx$,
and $\beta_{j,k} = \int f_j(x) 2^{\frac{j}{2}} \psi(2^j x - k) dx$.

Equation (8) expresses that the functions $2^{j/2}\phi(2^j x - k), k \in Z$, form an orthonormal basis. The decomposition of equation (8) is very flexible and decomposition of the fingerprint images result in orthogonal sub-bands. The resulting sub-bands are processed independently.

The 2-D wavelet transform is computed by applying 1-D algorithm over all the rows as well as columns of the input 2-D vector. Offsets are added and wavelet vector dimensions are adjusted. Thus, implementation of 2-D transform comes from the 1-D transform [14].

3) Maxima energy extraction: When an image is translated using these analysis wavelet filters, the decomposition coefficients associated with these filters for this image get modified instead of undergoing similar translation. However, the maxima of the wavelet transform also undergoes translation, when an image is translated [15]. Because of this, the wavelet maxima energy points are capable of detecting sharp variation points, and of formulating a signal presentation that is well adapted for characterizing patterns.

So, the first step performed after transforming the images is 'maxima energy extraction' for each scale. Let $\psi(x) \in L^2(R)$ be a function whose average is zero and

$$\psi_{2^j}(x) = \frac{1}{2^j} \psi(\frac{x}{2^j}) \quad (9)$$

The wavelet transform of a function $f(x)$ at the scale 2^j and position x can be viewed as the convolution product:

$$W_{2^j} f(x) = f * \psi_{2^j}(x) \quad (10)$$

The dyadic wavelet transform is the sequence of functions $(W_{2^j} f(x))_{j \in Z}$. After the transform, the sub-bands are marked, and n maxima values are retained for each scale.
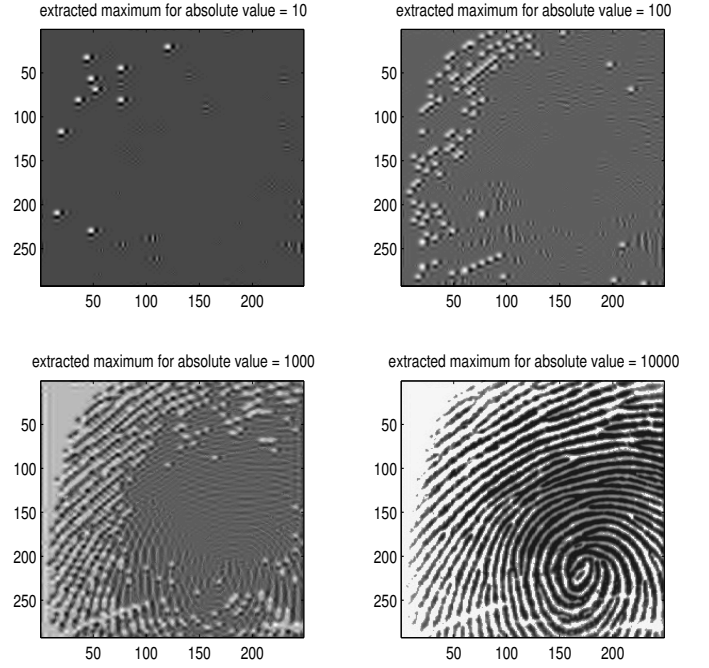

Fig. 5. Maxima energy extraction. The figure shows the inverse transform of sample fingerprint images after retaining the most significant 10,100,1000 and 10000 wavelet coefficients for each scale.

Figure (5) shows reconstructed fingerprint images after maxima energy extraction for different values of n, including 10, 100, 1000, and 10000, where n is the number indicating the total number of top values to be retained. The figure is generated by calculating the inverse transform from only the retained top n wavelet coefficients for each scale. For this algorithm, the value of n is chosen to be 10000.

4) Multiresolution analysis: Multiresolution analysis (MRA) can analyze the image under consideration at different scales simultaneously. This analysis mainly focuses on the low frequency content of the images. As the scale increases the image gets more blurred, adding to the low pass effect. For varying scales, by selecting the appropriate type of analysis filters, segmentation into horizontal, vertical, and diagonal directions is possible. Figure (6) displays the images with the details embedded for varying scales [14], [16].

While analyzing $2^n \times 2^n$ images, the maximum decomposition that is possible is scale n. The basis applied for the scale is determined as follows:

- Decompose given image into sub bands.
- Calculate energy of each sub band and get maximum energy value e_{max} for that scale. For a sub band $f(x,y)$ with $1 < x < X$, and $1 < y < Y$, energy is defined as

$$e = \frac{1}{XY} \sum_{x=1}^{X} \sum_{y=1}^{Y} |f(x,y)| \quad (11)$$

- If energy of a sub band is significantly small, such that $e < C \times e_{max}$, where C ranges from 0 to 1, stop the decomposition process. In this algorithm the criteria for stopping decomposition is that the energy content must be less than 40% of the total energy (C=0.4).
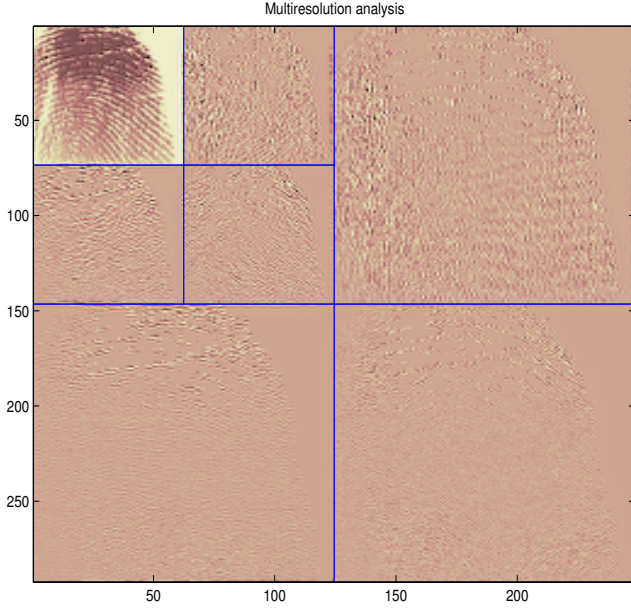
Fig. 6. Multiresolution analysis of a sample fingerprint image. The scale used is 2. The low pass band is seen in the left top corner. MRA mainly analyzes low pass contents of the image.

For this study the scale selected for MRA is 2. Within the second scale, four sub-bands are obtained, namely, low pass (LP), high pass (HP) diagonal, HP vertical and HP horizontal. These sub-bands are processed independently and are used for further analysis.

5) 2-D wavelet packet analysis: This technique performs analysis on both high pass as well as low pass content. The basis selection is done in such a way so as to suppress low pass content, and to enhance and analyze high pass content.

Wavelet packet expansion can be seen as algorithmically similar to a sub-band coding scheme. The entire collection of wavelet packets is matched effectively to the images for analysis and synthesis. An entropy based wavelet packet expansion called Coifman-Wickerhauser algorithm is used [17].

The core wavelet packet design comes from the basic quadrature mirror filter (QMF) bank [17]. The algorithm works as follows:

- Construct a vector containing the tree path as determined through the filter bank tree [15]. The filter associated with the tree path is interpolated using $2^{i-1} - 1$ zeros between each sample. The value of i ranges from $2^j - 1$ and selects one node of j branch tree.
- Interpolate and iterate the filters using the selected tree path, specified zeros, and selected scale.

For the specified or calculated basis, a wavelet packet transform is implemented. The algorithm works as follows:

- Perform level analysis in the analysis tree. The weight is calculated at every node. The output at every level is divided into high pass and low pass information content. For this particular algorithm, as further iterations are to be computed on high pass data, low frequency data is suppressed.
- Calculate points of division in accordance with the basis

vector tree developed.
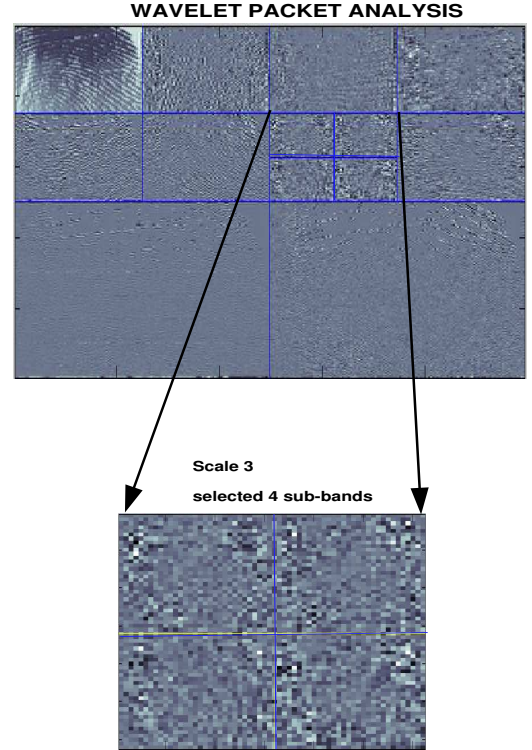- Zero pad the output, if necessary, to maintain the overall phase of the signal.

Fig. 7. Wavelet packet transform. The scale selected is 3, and all the sub-bands are shown. Only high pass scale 3 sub-bands are retained for further analysis. These are seen as the smallest four rectangles in the figure and magnified below.

Wavelet packet analysis of the image under consideration using selected basis is shown in figure (7). The designed tree and the corresponding wavelet packet sub bands are shown in figure (8). The figure demonstrates wavelet packet transform for three scales. All the wavelet bands are seen clearly. The low pass data, seen in the top left corner is discarded. The bands of interest are the four smallest rectangles used for further analysis. Although most of the energy spectrum is observed associated with the low frequency band, the fast changing coefficients are embedded in the high frequency band.

For this algorithm, norm values are used to calculate the weights of the node, and thus to formulate the basis vector. The selection process is same as the one described in the last section for the case of MRA. The scale selected for this analysis is 3. The best basis selected for the first image is used for the second image, such that there are similar sub-band divisions, in order to avoid any mismatch during further processing. The sub-bands from scale 3 are retained for further analysis.

C. Post-processing steps

Post-processing includes sub-band alignment, first difference and thresholding, and energy distribution analysis.
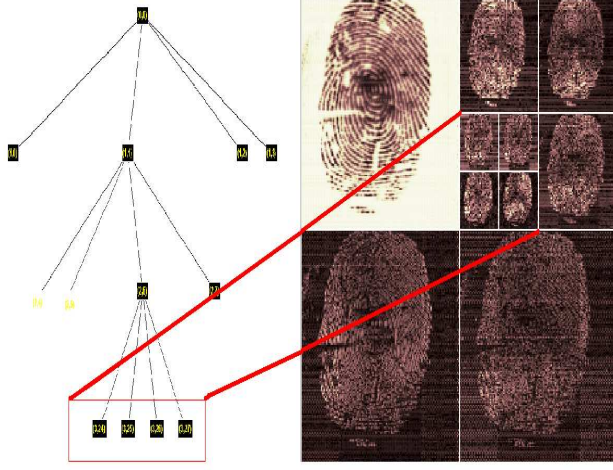
Fig. 8. An example of tree design using the best basis search and the corresponding wavelet packet decomposition of images. The four sub-bands at the end of the third scale are selected for further analysis. The basis is designed for every subject. The same basis is used for first and second images of the same subject.

1) Sub-band alignment: This step is essential in order to match coefficients in the correct sub-bands. The analysis is sub band oriented for wavelet packets and multiresolution analysis, such that all of the sub bands are processed separately. This alignment maintains the phase of the input signal throughout the process. To equate the lengths of the input and output sub-band vectors, either zero padding is implemented or alternate deletion is performed, where the band energy maxima is kept at the center. This protects significant coefficients in the case of over-loaded output sub-bands.

This particular step is important for Ethentica images. Since the size of Ethentica images is 315×240, the chances of mismatched sub-bands are high. The images captured by the other scanners are 248×292 in dimension, where the chances of mismatch are comparatively less.
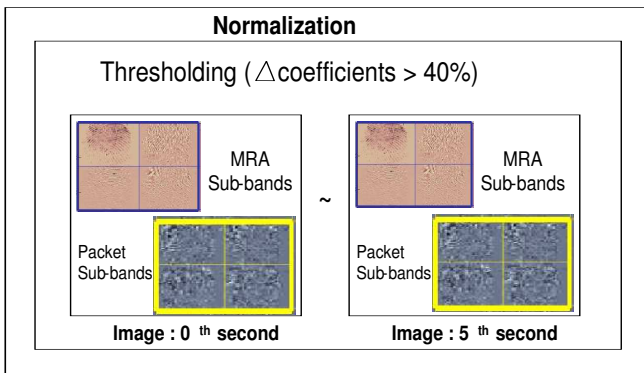

Fig. 9. Algorithm snap shot is shown with the elements arranged hierarchically from inside to outside. Selected sub-bands for MRA and wavelet packets are shown for both the images. It can be seen that differencing, thresholding and normalization follows after sub-band analysis of wavelet coefficients.

2) Threshold selection: The 'first' and 'second' images are decomposed using the MRA scheme and by the wavelet packet scheme as discussed previously. The 2nd scale of MRA and

3rd scale of wavelet packets are the sub-bands which are retained for both the images. The first difference of the first and second images is taken in the individual sub-bands. Normally singularities are not very obvious in images, nor are they reflected in the wavelet coefficients. Therefore, non-significant coefficients of the discrete wavelet transform are discarded and the remaining are enhanced, through thesholding. The threshold value is used to decide whether a coefficient has experienced significant change. Each coefficient is retained if it changes more than 40%, from the first to the second image. Coefficients which do not change more than 40% are discarded. This value was selected through brute force method.

The operation of closing is performed on the image captured at zeroth second, and then the image is inverted. The energy content of the difference image is retained if the image captured at the zeroth second correspondingly has a non-zero value associated with it. This is essential to avoid false energy increments for the case of fingerprints spreading. Figure (9) gives a combined view of the post processing part of the algorithm. Figure (10) shows reconstructed images from the changing wavelet coefficients and demonstrates how the perspiration pattern has been isolated.
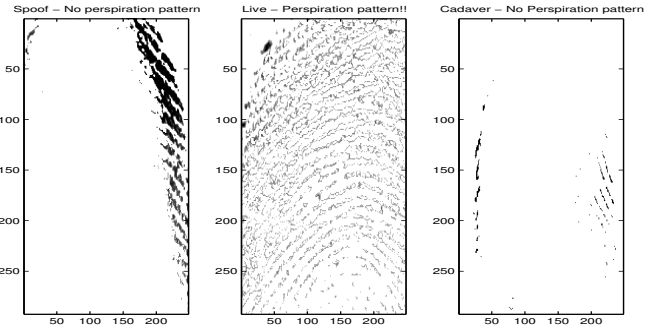

Fig. 10. Perspiration patterns. Spoof, live, and cadaver patterns are shown from left to right. The perspiration pattern is the reconstruction of the isolated wavelet coefficients obtained by the algorithm described in this paper. The perspiration pattern is observed only in the case of live finger. The energy due to spreading effect for spoof and cadaver images is removed as described in the threshold selection step.

3) Energy distribution analysis: The total energy associated with the changing wavelet coefficients, determined as described in the previous section, normalized by total energy for 5 second image, is used as the measure to decide liveness. The equation is as follows:

$$e\% = (\frac{\sum \text{energy of sub bands of difference image}}{\sum \text{energy of sub bands of last image}}) \times 100 \tag{12}$$

A training data set is used to determine the threshold value for all the scanners. Results are formulated using testing data set. Classification was performed using two categories: live and not live (spoof and cadaver).

III. RESULTS

This section shows the results generated after applying the algorithm to a dataset of live, spoof, and cadaver fingerprint images, described previously.
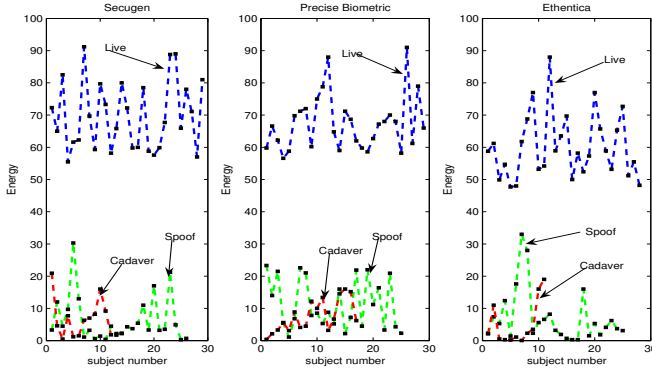
Fig. 11. Training data set results for Secugen, Precise Biometrics and Ethentica images, from left to right, when the time between images is 5 seconds. Top lines are for live subjects and bottom lines are for spoof/cadaver subjects.

A. Energy distribution analysis

The total energy associated only with the changing coefficients normalized by the second images is calculated, in order to determine the liveness associated with the finger. Figures (11) and (12) show the results for the training and testing data sets, respectively, when the second image is captured after 5 seconds. The training and testing data set results for the second image captured after 2 seconds are given in figures (13) and (14), respectively.
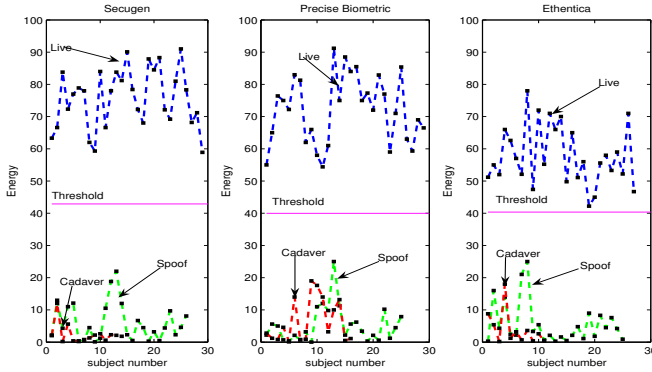

Fig. 12. Testing data set results for Secugen, Precise Biometrics and Ethentica images, from left to right, when the time between images is 5 seconds. Top lines are for live subjects and bottom lines are for spoof/cadaver subjects. The threshold is determined from the training set.

B. Threshold selection

Since there is no overlap between the energy content distributions of live and cadaver/spoof distribution, we can perfectly separate the two groups using a threshold based on the training set that falls between the maximum of the cadaver/spoof distribution and the minimum of the live distribution. This is true for all three types of scanners. The different threshold values selected for different scanners, for both 5 second and 2 second categories are given in table (III).

For the testing data set, perfect classification is achieved using the threshold values.

TABLE III
THRESHOLD SELECTION BASED ON TRAINING SET

Scanner category	Time window	Live min energy	Non-live max energy	Threshold level
Secugen	5 sec	55.5	30.3	**42.9**
Secugen	2 sec	41.8	27.3	**34.55**
Precise	5 sec	56.6	23.3	**39.97**
Biometrics	2 sec	42.0	21.2	**31.6**
Ethentica	5 sec	47.7	33.0	**40.35**
Ethentica	2 sec	48.6	28.0	**38.3**

IV. DISCUSSION AND FUTURE WORK

A new wavelet based method has been developed which is based on detecting perspiration pattern from a time-series of fingerprint images measured directly from scanner. This method calculates wavelet coefficients which characterize perspiration changes in live fingers, thus separating them from spoof or dismembered fingers. Wavelet packet and multiresolution analysis isolate the perspiration changes and total energy, given in equation (12), is used as a measure to decide liveness. Threshold values, based on the energy distribution of the training data, were found to be capable of completely classifying the test data into two classes: live and not live. This phenomenon was observed for three fingerprint scanners given in table (I) and for both $2s$ and $5s$ time windows.
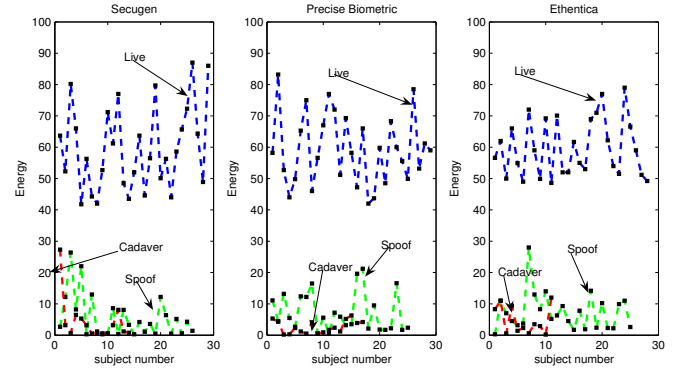

Fig. 13. Training data set results for Secugen, Precise Biometrics and Ethentica images, from left to right, when the time between images is 2 seconds. Top lines are for live subjects and bottom lines are for spoof/cadaver subjects.

Previous algorithms to quantify perspiration for liveness are given in [4], [8] and enhanced in [11]. While these algorithms were able to achieve approximately 90% classification, the presented algorithm was able to completely classify live fingers from not live fingers. Also, this algorithm was tested using a larger database than used previously. The effectiveness of the algorithm was shown for both $5\ second$ and $2\ second$ time windows.

Liveness detection has been suggested as a countermeasure against spoofing of fingerprint scanners. Previously, to strengthen fingerprint recognition, several liveness measures including pulse, pulse oximetry, electrocardiogram, temperature detection and multi-spectroscopy based techniques are suggested [18], [19], [20], [21], [6], [5], [9], [7], [10], [22], [23]. Pulse oximetry is based on differential absorption of
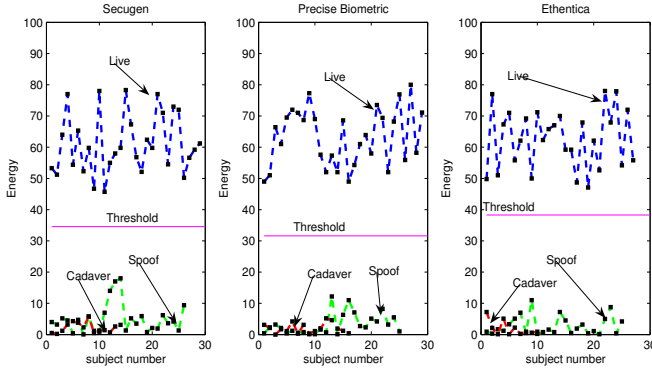
Fig. 14. Testing data set results for Secugen, Precise Biometrics and Ethentica images, from left to right, when the time between images is 2 seconds. Top lines are for live subjects and bottom lines are for spoof/cadaver subjects. The threshold is determined from the training set.

two wavelengths of light projected through the finger. While blood oxygen content is ignored, the pulse information is used for liveness detection. This method suffers with drawbacks like the requirement that the finger be completely covered for the test since ambient light may interfere. Another suggested method is an electrocardiogram (ECG) measurement. This methods requires two contact points on the opposite sides of the subject's body to be able to perform the measurement, is bulky, and hence less practical. An elegant approach uses multi-spectral sensors to expose the finger to different optical wavelengths. This, as in others, requires extra hardware in a specially designed fingerprint scanner. Also, it may be possible that semitransparent faux fingers, covering only the fingerprint surface, can be made with precision, and these techniques can be spoofed. The proposed method, being purely software based, is cheaper and more flexible for future adaptations.

As the physiological phenomenon of perspiration is at the base of the detection process, it would be interesting to study variations in the perspiration, and how the algorithm behaves for those variations. While the algorithm is shown to give 100% classification for the limited data used, more data with multiple scanners and with different underlying technologies is required to validate the perspiration phenomenon across the population and also validate the capabilities of the presented work. It is desired to test the performance of the algorithm under different environmental settings including hot weather, cold weather and different finger conditions including dirty fingers, wet fingers and dry fingers. The algorithm can be evaluated in the light of the fact that the above conditions are problematic for performing the fingerprint recognition, irrespective of liveness detection.

More testing needs to be performed to discover ways to spoof the liveness algorithm, including using pressure variability and additional moisture. The data collected from the live subjects was performed for normal conditions with no additional requirements to prevent natural movements. Various image enhancement techniques used in this work, make the algorithm more immune to non-deliberate distortions, varying pressures and other noise elements present at the time of fingerprint capture. The algorithm uses wavelet packet analysis, which formulates the basis using Shannon entropy, to arrange the ridge information in the order of significance, thus making the wavelet based algorithm less prone to deliberate distortion attempts.

Certain portions of the algorithm like basis formation, threshold selection and filter design need attention to improve the algorithm. While testing the algorithm for more severe conditions, fuzzy partitioning can be employed instead of hard thresholding to improve the sensitivity of the system. Basis selection can be made more efficient by learning the perspiration pattern characteristics. Reduction of the time between images should be studied. Presently two seconds was the minimum time tested. Since commercial devices were used, this was the minimum allowed by the device SDKs. Initial evidence has indicated this time could be significantly decreased.

Lastly the algorithm is developed using MATLAB 6.5, with a pentium processor, with 1GB RAM. The entire algorithm takes roughly 2 seconds, excluding image capture time, to formulate results for each subject, thus making it unsuitable for on-line use. Converting the developed algorithm to more basic level languages like C, Fortran, or assembly level language would improve the speed. Other methods to simplify the algorithm may need to be considered including filter design and selection of faster wavelets like bi-orthogonal wavelet using lifting scheme.

V. CONCLUSION

A new approach to detect liveness associated with fingerprint scanners is proposed. The approach is based on detection of a perspiration pattern from two successive fingerprints captured at zeroth second and after two or five seconds. The algorithm combines the use of Daubechies wavelet transform, multiresolution analysis, and wavelet packet transform techniques to isolate the changing energy of the perspiration pattern. The energy distribution of the changing coefficients is used as a measure to perform classification. As there is no overlap between energy distribution of live fingers and not live fingers, the classification is straightforward. A threshold selected from the training set gives perfect separation for the test set. This method is tested for three different types of scanner technologies, namely optical, opto-electrical, capacitive DC. Advantages of this method are that it is purely software based, no hardware enhancements are required, and hence is economical.

ACKNOWLEDGMENT

REFERENCES

[1] J. D. Woodward, N. M. Orlans, and P. T. Higgins, *Biometrics*. McGraw-Hill/Osborne, 2003.

[2] A. Jain, R. Bolle, and S. Pankanti, *Biometrics: Personal Identification in Networked Society*. Kluwer Academic Publisher, 1999.

[3] D. Maltonie, D. Maio, A. K. Jain, and S. Prabhakar, *Handbook of Fingerprint Recognition*. Springer-Verlag New York, Inc., 2003.

[4] S. Schuckers, "Spoofing and anti-spoofing measures," in *Information Security Technical Report*, vol. 7, 2002, pp. 56–62.

[5] T. Matsumoto, H. Matsumoto, K. Yamada, and S. Hoshino, "Impact of artificial 'gummy' fingers on fingerprint systems," in *Proceedings of SPIE*, vol. 4677, Jan 2002.

[6] T. Putte and J. Keuning, "Biometrical fingerprint recognition: don't get your fingers burned," in *Smart Card Research and Advanced Applications*. Kluwer Academic Publisher, 2000, pp. 289–303.

[7] D. Willis and M. Lee, "Biometrics under our thumb," *Network Computing*, June 1998.

[8] R. Derakshani, S. Schuckers, L. Hornak, and L. Gorman, "Determination of vitality from a non-invasive biomedical measurement for use in fingerprint scanners," *Pattern Recognition Journal*, vol. 36, no. 2, 2003.

[9] L. Thalheim and J. Krissler, "Body check: biometric access protection devices and their programs put to the test," *c't magzine*, Nov 2002.

[10] V. Valencia and C. Horn, "Biometric liveness testing," in *Biometrics*. McGraw-Hill/Osborne, 2003.

[11] S. Parthasaradhi, R. Derakshani, L. Hornak, and S. Schuckers, "Time-series detection of perspiration as a liveness test in fingerprint devices,," *IEEE Transactions on Systems, Man, and Cybernetics, Part C: Applications and Reviews,*, vol. 36, no. 2, 2005.

[12] I. Daubechies, *Ten Lectures on Wavelets*. Society of Industrial and Applied Mathematics, 1998.

[13] I. Daubechies, Y. Meyer, P. G. Lemerie-Rieusset, P. Techamitchian, G. Beylkin, R. Coifman, M. V. Wickerhauser, and D. Donoho, "Wavelet transform and orthonormal wavelet bases," in *Different Perspectives on Wavelets*, vol. 47, San Antonio, Texas, Jan. 1993, pp. 1–33.

[14] Y. Meyer, *Wavelets: Algorithms and Applications*. Society of Industrial and Applied Mathematics, 1993.

[15] M. B. Ruskai, G. Beylkin, R. Coifman, I. Daubechies, S. Mallat, Y. Meyer, and L. Raphael, "Wavelet transform maxima and multiscale edges," in *Wavelets and Their Applications*, Lowell, Massachusetts, 1992, pp. 67–104.

[16] I. Daubechies, Y. Meyer, P. G. Lemerie-Rieusset, P. Techamitchian, G. Beylkin, R. Coifman, M. V. Wickerhauser, and D. Donoho, "Best-adapted wavelet packet bases," in *Different Perspectives on Wavelets*, vol. 47, San Antonio, Texas, Jan. 1993, pp. 155–171.

[17] M. B. Ruskai, G. Beylkin, R. Coifman, I. Daubechies, S. Mallat, Y. Meyer, and L. Raphael, "Wavelets and filter banks for discrete-time signal processing," in *Wavelets and Their Applications*, Lowell, Massachusetts, 1992, pp. 17–52.

[18] D. Osten, H. Carim, M. Arneson, and B. Blan, "Biometrics, personal authentication system," *US Patent #5,719,950*, Feb 1998.

[19] K. Seifried, "Biometrics - what you need to know," *Security portal*, Jan 2001.

[20] P. Lapsley, J. Less, D. Pare, and N. Hoffman, "Anti-fraud biometric sensor that accurately detects blood flow," *US Patent #5,737,439*, April 1998.

[21] P. Kallo, I. Kiss, A. Podmaniczky, and J. Talosi, "Detector for recognizing the living character of a finger in a fingerprint recognizing apparatus," *US Patent #6,175,64*, Jan 2001.

[22] S. Kurt, "Biometrics - what you need to know," *Security Portal 10*, Jan 2001.

[23] K. A. Nixon and R. K. Rowe, "Spoof detection using multispectral fingerprint imaging without enrollment," in *Proceedings of Biometric Symposium*, Sept 2005.

Stephanie Schuckers (M'95) received the M.S. and Ph.D. degrees in electrical engineering from the University of Michigan, Ann Arbor, in 1994 and 1997 respectively, where she was a Whitaker Foundation Graduate Fellow.

Currently, she is an Associate Professor with the Department of Electrical and Computer Engineering, Clarkson University, Potsdam, NY. Her primary research interest is the application of modern digital signal processing and pattern recognition to biomedical signals. Signals include the electrocardiogram, biometric signals like fingerprints, pulse oximetry, respiration, and electrocephalograms. Her work is funded by various sources, including National Science Foundation, American Heart Association, National Institute of Health, and private industry.

Aditya Abhyankar received the BE degree in Electronics and Telecommunication Engineering from Pune University, India in 2001. He received the MS and Ph.D. degrees from Clarkson University, NY, USA in 2003 and 2006 respectively. He worked as a post-doctoral fellow at Clarkson University, NY, USA in the academic year 2006-07. He worked as a consultant for Biometrics LLC, WV, USA in 2007. Currently he works as a Research Associate at Clarkson University and Professor at Computer Engineering Department of Vishvakarma Institute of Information Technology (VIIT), Pune. He works as Dean of R&D and Director of CERD (Center for Excellence in Research and Development) at VIIT, Pune. He is also associated as Adjunct Professor with Government College of Engineering, Pune (COEP). He is involved in consultancy with number of private industries. His research interests include signal and image processing, pattern recognition, wavelet analysis, biometric systems and bioinformatics.